

Predicting Inter-session Performance of SMR-Based Brain–Computer Interface Using the Spectral Entropy of Resting-State EEG

Rui Zhang · Peng Xu · Rui Chen · Fali Li ·
Lanjin Guo · Peiyang Li · Tao Zhang ·
Dezhong Yao

Received: 19 October 2014 / Accepted: 26 February 2015 / Published online: 19 March 2015
© Springer Science+Business Media New York 2015

Abstract Currently most subjects can control the sensorimotor rhythm-based brain–computer interface (SMR-BCI) successfully after several training procedures. However, 15–30 % of subjects cannot achieve SMR-BCI control even after long-term training, and they are termed as “BCI inefficiency”. This study focuses on the investigation of reliable SMR-BCI performance predictor. 40 subjects participated in the first experimental session and 26 of them returned in the second session, each session consists of an eyes closed/open resting-state EEG recording run and four EEG recording runs with hand motor imagery. We found spectral entropy derived from eyes closed resting-state EEG of channel C3 has a high correlation with SMR-BCI performance ($r = 0.65$). Thus, we proposed to use it as a biomarker to predict individual SMR-BCI performance. Receiver operating characteristics analysis and leave-one-out cross-validation demonstrated that the spectral entropy predictor provide outstanding classification capability for high and low aptitude BCI users. To our knowledge, there has been no discussion about the reliability of inter-session prediction in previous studies. We further evaluated the inter-session prediction performance of the spectral entropy predictor, and the results showed that the average classification accuracy of inter-session prediction up to 89 %. The proposed predictor is convenient to obtain

because it derived from single channel resting-state EEG, it could be used to identify potential SMR-BCI inefficiency subjects from novel users. But there are still limitations because Kübler et al. have shown that some BCI users may need eight or more sessions before they develop classifiable SMR activity.

Keywords Brain–machine interface (BMI) · Resting-state EEG · BCI inefficiency · Biomarker · Classification

Introduction

The rapid development of neuroscience provides a window for scientists to deeply understand the human brain, meanwhile the acquired knowledge provides opportunities to further extend the normal function of human brain. Brain–computer interface (BCI) is such a technology which translates the intent of a human brain directly into control commands without involving peripheral neural pathways (Wolpaw et al. 2002). Many augmentative communication and control systems based on BCI have been developed (Donchin et al. 2000; Li et al. 2010; Wang et al. 2006; Wolpaw and McFarland 2004). Among them, sensorimotor rhythm-based BCI (SMR-BCI) has received a lot of attentions in recent years due to its potential applications in neurological rehabilitation and in assisting patients with impaired motor functions (Daly and Wolpaw 2008; Gongora et al. 2013).

Over the past ten years, effective feature extraction and pattern recognition algorithms have been applied to the SMR-BCI system to shorten training time and increase information transfer rates (Lotte and Guan 2011; Lu et al. 2012; Vidaurre et al. 2011; Xu et al. 2014; Zhang et al. 2013). Although these algorithms have significantly

R. Zhang · P. Xu (✉) · R. Chen · F. Li · L. Guo · P. Li ·
T. Zhang · D. Yao (✉)
Key Laboratory for NeuroInformation of Ministry of Education,
School of Life Science and Technology, University of Electronic
Science and Technology of China, No. 4, Section 2, North
Jianshe Road, Chengdu, China
e-mail: xupeng@uestc.edu.cn

D. Yao
e-mail: dyao@uestc.edu.cn

improved SMR-BCI control performance at the level of individual subject, the inter-subject variations remain a substantial problem requiring additional investigation (Noted that the subject mentioned here is healthy subject, not patient). In a recent study, 30 out of 80 (37.5 %) healthy subjects were unable to achieve a classification accuracy of or above 70 %, which is considered the lower threshold for reliable communication (Hammer et al. 2012). In another earlier study published in 2003, the percentage of subjects achieving a classification accuracy below 70 % was even greater (48.7 %) (Guger et al. 2003). Therefore, it is of great significance to find reliable physiological biomarkers to predict individual SMR-BCI performance (Blankertz et al. 2010), the development of predictors could identify the potential SMR-BCI inefficient subjects, helping them to avoid the frustrating and costly training procedures. On the other hand, the related study may in turn be instructive for the establishment of enhanced training strategies for those low performance subjects (Vidaurre and Blankertz 2010).

Several variables, including psychological measures, neuroanatomical and neurophysiological features, have been proposed to elucidate the neural mechanisms accounting for the variations in SMR-BCI performance in recent years. Hammer et al. calculated correlations between online classification accuracy of SMR-BCI and a variety of psychological tests, including measures of visuo-motor coordination, attention span, intelligence, and verbal as well as non-verbal learning abilities (Hammer et al. 2012). They found that visuo-motor coordination skills and the ability to concentrate on a task both exhibited significant positive correlations with classification accuracy of SMR-BCI ($r = 0.42$ and $r = 0.50$, respectively). Vuckovic et al. revealed that the score of kinaesthetic motor imagery questionnaires is correlated well with SMR-BCI classification accuracy ($r = 0.53$) (Vuckovic and Osuagwu 2013). Halder et al. studied the link between white matter architecture and SMR-BCI performance, their results demonstrated that the structural integrity and myelination quality of the deep white matter structures, such as the corpus callosum, cingulum, and superior fronto-occipital fascicle, are positively correlated with individual SMR-BCI performance (Halder et al. 2013). They also investigated the fMRI activation differences between user groups with high and low SMR-BCI performance, and found that high performance SMR-BCI users exhibit larger activations in the supplementary motor area (SMA) and right middle frontal gyrus during motor observation (Halder et al. 2011).

Currently, scalp EEG is the main source signal for the SMR-BCI, thus it would be meaningful to identify EEG-related biomarkers correlated with the variations of SMR-BCI performance. Blankertz et al. presented that the amplitude of the SMR during rest is positively correlated with

subsequent online SMR-BCI classification accuracy (Blankertz et al. 2010). Their results also indicated that SMR-BCI performance could be improved by enhancing the amplitude of the resting-state SMR. Ahn et al. reported that high theta and low alpha waves during rest were observed for those subjects with low SMR-BCI performance (Ahn et al. 2013). Grosse-Wentrup et al. investigated the variations of SMR-BCI performance within a single session and found that high-frequency gamma oscillations originating in fronto-parietal networks could predict the trial-to-trial performance variations (Grosse-Wentrup and Schölkopf 2012). The existing EEG-based studies revealed that subject's SMR-BCI performance is related with the power spectrum of low frequency resting-state EEG. It has been proved that entropy is capable of capturing the complexity in a series (Inouye et al. 1991; Xu et al. 2013a). Thus, entropy may be used to capture the complexity in the power spectral density (PSD) of the resting-state EEG, which may provide a new measure to predict SMR-BCI performance.

In the current study, we proposed to use spectral entropy of the resting-state EEG as a biomarker to predict individual SMR-BCI performance, and compared its prediction performance with SMR predictor (Blankertz et al. 2010) and alpha-theta ratio (ATR) predictor (Ahn et al. 2013).

Materials and Methods

Experimental Setup

A total of 40 subjects (15 females, aged 21.7 ± 2.6 years, three left-handed) participated in the experiment. All participants were asked to read and sign an informed consent form before participating in the study. After the experiment, all participants received monetary compensation for their time and effort.

The experiment consisted of two sessions. All 40 subjects participated in the first session. Among them, 26 subjects returned to participate in the second session, and the tasks in the two sessions were the same.

The subjects sat in a comfortable armchair 90 cm in front of a computer screen. They were instructed not to move and to keep both arms relaxed. Fifteen Ag/AgCl electrodes (F3, F4, FC3, FC4, Cz, C3, C4, C5, C6, CP3, CP4, P3, P4, O1, O2) from extended 10–20 system were selected for EEG recording by using a Syntop amplifier (Syntop Instrument, Beijing, China). AFz electrode was adopted as reference, and the signal were sampled at 1000 Hz and band-pass filtered between 0.5 and 45 Hz.

Each experimental session started with a recording of the resting-state EEG, including 1 run in which the subjects rested with their eyes open and 1 run rested with their eyes

closed. The recording sequence for these two rest runs was randomly balanced among the subjects. Each recording run lasted 2 min, with a 2 min break between runs.

Following a 2 min break, the motor imagery dataset including four runs was recorded. The subjects were asked to perform motor imagery with left or right hand according to the instructions appearing on the screen (see Fig. 1b). Each trial started with a 4 s rest period. A yellow bar then appeared on the left or right side of the screen for 1 s to instruct the subjects to use their left or right hand to perform motor imagery. After the bar turned green, subjects started to perform the requested hand motor imagery, which lasted 5 s. The order of the left and right bars was randomized, and the duration of each trial was 10 s. There were 50 trials per run and approximately 25 trials for each motor imagery condition, and there was a 2 min break between the consecutive two runs. In total, each participant performed 200 motor imagery trials.

Approximately 3 months after this first session, 26 of the 40 subjects returned to repeat the same experiments under the same recording conditions and procedures. All datasets of the two sessions were saved for further analysis.

SMR-BCI Performance

The SMR-BCI performance of all subjects was obtained from their motor imagery datasets and characterized by the SMR-BCI recognition rate. It was evaluated by using the first 2 runs in the motor imagery dataset as the training set and the last 2 runs as the test set.

During the training process, all the EEG segments during hand motor imagery were selected for analysis, and those trials with absolute amplitude above $100 \mu\text{V}$ were considered to be contaminated with artifacts and will be removed from the following analysis. Next, the EEG segments were filtered by a subject-specific optimal band-pass filter, which was obtained by r^2 as below,

$$r^2 = \left(\frac{\sqrt{L_1 L_2} \text{mean}(X_1) - \text{mean}(X_2)}{L_1 + L_2 \text{std}(X_1 \cup X_2)} \right)^2 \quad (1)$$

where X_1 and X_2 are task-related power spectrum of the two classes motor imagery EEG data, and L_1 and L_2 are the number of trials in the two corresponding classes. The value of r^2 reflects the difference in the power of the two classes, with the larger r^2 value denoting the greater difference between the two classes. The band-pass filtered EEG signal were then transferred to three pairs of optimal spatial filters, estimated by common spatial patterns (CSP) method for each subject (Müller-Gerking et al. 1999). The logarithm transformation of the variance of the spatially filtered signal, resulting in a six-dimensional feature vector, was used as the final features. Linear discriminate analysis (LDA) was used as the classifier for task recognition, in order to discriminate it from the LDA classifier mentioned in Sect. 2.4, we named it as decoding-LDA. In the end of the training procedures, the decoding-LDA classifier was trained by the labeled features extracted from the training set, and the trained classifier was then used for task recognition on the test dataset.

For the test process, the same band-pass and spatial CSP filters determined from the training dataset were used to filter the EEG signal at first. Then the 6-dimensional log-variance of the filtered EEG signal was transferred to the trained decoding-LDA classifier to perform the final recognition.

Spectral Entropy

Spectral entropy, derived from Shannon entropy, quantifies the spectral complexity of a time series. Based on the disparate information hidden in the spectrum of the resting-state EEG, as reported in previous studies (Ahn et al. 2013; Blankertz et al. 2010), we proposed to use spectral entropy to build the biomarker for SMR-BCI performance.

The calculation procedures were shown in Fig. 2. We discarded the first and last 10 s of data from the 2 min resting-state EEG recording for each subject and divided the remaining 100 s data into 10 segments, with 10 s data per segment. The power spectral density (PSD) $P(f)$ of each

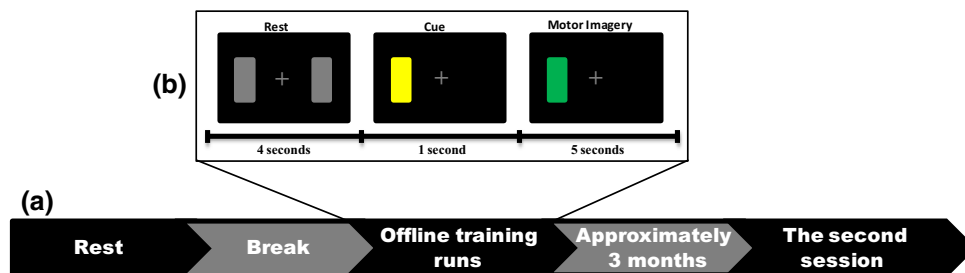


Fig. 1 EEG experimental paradigm. **a** Recording sequence for the experiment. **b** Offline experimental paradigm for one trial, consisting of the following: a 4 s rest period, indicated by both side gray bars; a

1 s cue, indicated by the left/right side yellow bar; and a 5 s motor imagery task, indicated by the left/right side green bar (Color figure online)

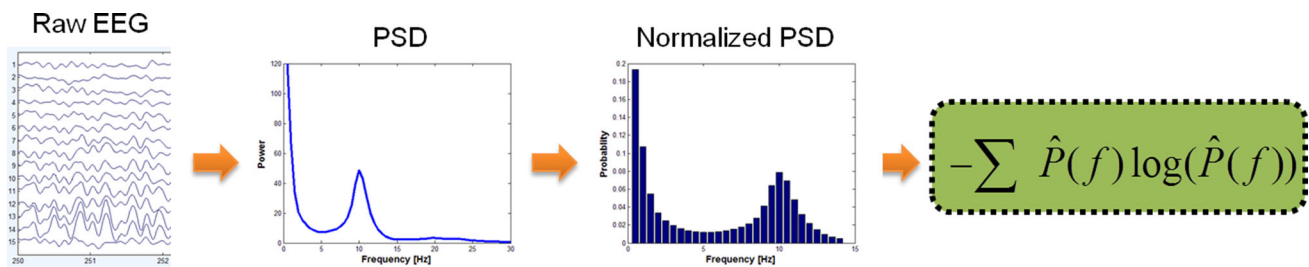


Fig. 2 The procedures for calculating spectral entropy

segment was estimated using Welch's method. The PSD represents the distribution of power as a function of frequency, and the normalization of $P(f)$ with respect to the total power yields a probability density function. In current work, we estimated spectral entropy based on the PSD within 0.5–14 Hz, and the corresponding normalization was determined by Eq. 2 so that $\sum_{f=0.5}^{f=14} \hat{P}(f) = 1$.

$$\hat{P}(f) = P(f) / \sum_{f=0.5}^{f=14} P(f) \quad (2)$$

Finally, the entropy of $\hat{P}(f)$ was calculated using the following equation:

$$SH = - \sum_{f=0.5}^{f=14} \hat{P}(f) \log(\hat{P}(f)) \quad (3)$$

where the base of the logarithm is two and the unit of SH is bits. In essence, spectral entropy represents the uniformity of PSD, the greater the spectral entropy, the more irregular the PSD distribution.

After the above procedures, ten 15-dimensional spectral entropy vectors (one dimension for one channel) were obtained for both eyes open and eyes closed resting-state EEG runs of each subject. Averaging the ten vectors yielded 15-length channel spectral entropies, and the relationships between those spectral entropies and SMR-BCI performance were analyzed in current study.

SMR-BCI Performance Prediction

Two groups of subjects were screened according to their SMR-BCI recognition rates, subjects who had achieved recognition rates above 80 % were assigned to the high aptitude SMR-BCI user group, and subjects with recognition rates below 70 % were assigned to the low aptitude SMR-BCI user group. The subject's spectral entropy derived from eyes closed resting-state EEG of channel C3 was selected to predict the corresponding SMR-BCI performance, that is discriminating the user group which it belonged to. LDA was used to build the prediction model, in order to discriminate it from the LDA classifier mentioned in Sect. 2.2, we named it as prediction-LDA. The

predictor was one-dimension since only channel C3 was selected, thus the classifier model could be denoted as a boundary.

In order to test the stability of the predictor's performance, we evaluated its prediction capability under intra- and inter-session situations, respectively. In the intra-session prediction, leave-one-out cross-validation scheme was used separately for the first and second sessions. One subject was selected as test sample, the rest of the subjects were considered as train samples for estimating the classification boundary, the above procedures were repeated until each subject has been assigned as test sample for one time and the prediction accuracy was equal to the percentage of correct classifications. During the inter-session prediction, subjects in the first session were first classified by the classification boundary estimated from the second session, and then subjects in the second session were classified by the classification boundary estimated from the first session.

Changes in SMR-BCI Performance and Predictors Between Sessions

For the same subject, SMR-BCI performance usually varied between the first and second sessions, therefore, we aimed to investigate whether the performance change could be reflected by the predictors obtained from the resting-state EEG. Because SMR-BCI performance and the predictors are of different scales, we defined a measurement named as change percentage (CP) for a fair comparison as,

$$CP = 2 \times (S2 - S1) / (S1 + S2) \times 100 \% \quad (4)$$

where $S1$ represents the SMR-BCI recognition rate, and the predictors for the same subject in the first session, and $S2$ represents them in the second session.

Related Work

Two important predictors based on resting-state EEG have been proposed recently. The first one was developed by (Blankertz et al. 2010), which was determined by the maximum difference between the PSD curve and a fit of

the $1/f$ noise spectrum, since the value estimated the strength of SMR, it was named as SMR predictor. The second one was proposed by (Ahn et al. 2013), which equaled to the ratio of alpha band (8–13 Hz) power and theta band (4–8 Hz) power, and it was named as ATR predictor in current study. We calculated the above two predictors from both the eyes closed and open resting-state EEG, and compared their prediction performance with the proposed spectral entropy predictor.

Results

SMR-BCI Performance

The SMR-BCI recognition rates calculated from session 1 (40 subjects) and 2 (26 subjects) were shown in Fig. 3. The average recognition rate of the two sessions was $72.9 \pm 14.1\%$ ($71.1 \pm 13.9\%$ for the first session and $75.7 \pm 14.3\%$ for the second session), and it is clear that the recognition rates covered the full range from chance-level performance (50 %) to completely control (100 %). Considering the performance of the 26 subjects who had returned to participate in the second session recording experiment, we found that the correlation coefficient (CC) between the recognition rates of the two sessions was 0.83 ($p < 10^{-6}$). Although the mean recognition rate in the second session was 3.7 % higher than that in the first session, this difference was not significant (two-sample t test, $p = 0.34$).

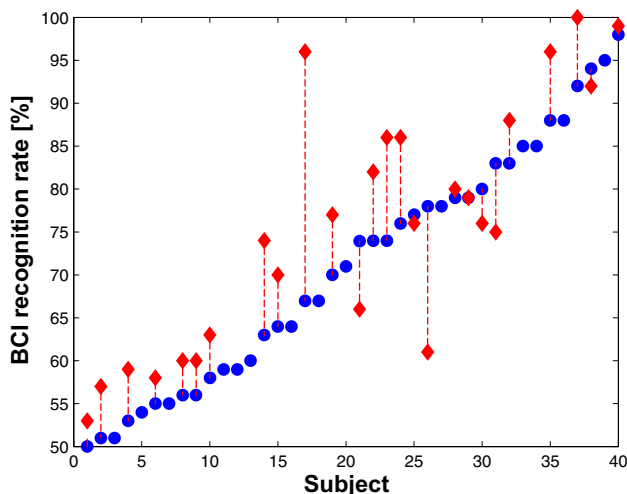


Fig. 3 Distribution of the SMR-BCI recognition rates in 40 subjects. Horizontal coordinate denotes the subjects, and vertical coordinate denotes their SMR-BCI recognition rates. The blue solid circles indicate SMR-BCI recognition rates in the first session, and the red solid diamonds indicate SMR-BCI recognition rates in the second session (Color figure online)

Correlations with SMR-BCI Performance

The CCs between the spectral entropies from the resting-state EEG recording and the SMR-BCI performance of the same session were firstly calculated across channels based on the merged session ($N = 66$), nine of 15 channels showed stronger correlation as presented in Fig. 4. The strongest correlation between the spectral entropy predictor and the SMR-BCI recognition rate was captured on channel C3 from the EEG recording during the resting-state with closed eyes ($r = 0.65$, $p < 10^{-8}$). Similarly in the two separate sessions, the highest CCs were also achieved by channel C3 from eyes closed resting-state EEG with $r = 0.61$ ($p < 10^{-4}$) for the first session, and $r = 0.70$ ($p < 10^{-4}$) for the second session. Therefore, the spectral entropy obtained from eyes closed resting-state EEG of channel C3 was chosen as the predictor in the following analysis, and the relationship between the predictor and the SMR-BCI performance was presented in Fig. 5a.

The strongest correlation between the SMR predictor and the SMR-BCI recognition rate was observed on channel C4 of the EEG recording during the resting-state with eyes open (Fig. 4), and Fig. 5b showed the detailed relationship with CC being 0.29 ($p = 0.02$). For ATR predictor, the strongest correlation was achieved on channel FC3 of eyes closed resting-state EEG (Fig. 4), and the scatter plot was illustrated in Fig. 5c with CC being 0.51 ($p < 10^{-4}$).

Intra-session Prediction

The first and second sessions were analyzed separately in this section. According to the grouping definition described in Sect. 2.4, 10(18) subjects were assigned to the high (low) aptitude SMR-BCI user group for the first session, while for the second session, the subject number of the high (low) aptitude SMR-BCI user group was 9(9). The receiver operating characteristic (ROC) analysis was firstly conducted to evaluate the classification capability of the proposed spectral entropy predictor for the two separate sessions, where high and low aptitude SMR-BCI users were defined as positives and negatives, respectively. As illustrated in Fig. 6, the resulting area under curve (AUC) was 0.89 for the first session and 0.90 for the second session. The optimal operating point was also found so that the proportions of misclassified positive and negative cases were the same. At the optimal operating point, the (sensitivity, specificity) were (0.90, 0.83) and (1.0, 0.78) for the first and second sessions, respectively.

Regarding to the SMR and ATR predictors, the AUCs were 0.57, 0.74 for the first session and 0.69, 0.80 for the second session (Fig. 6). At the optimal operating point, the (sensitivity, specificity) were (0.40, 0.89), (0.50, 0.94) for

Fig. 4 Correlations between the three predictors and SMR-BCI performance. *Green line* denotes the spectral entropy predictor; *blue line* denotes the SMR predictor; and *red line* denotes the ATR predictor. Left eyes closed resting-state; right eyes open resting-state (Color figure online)

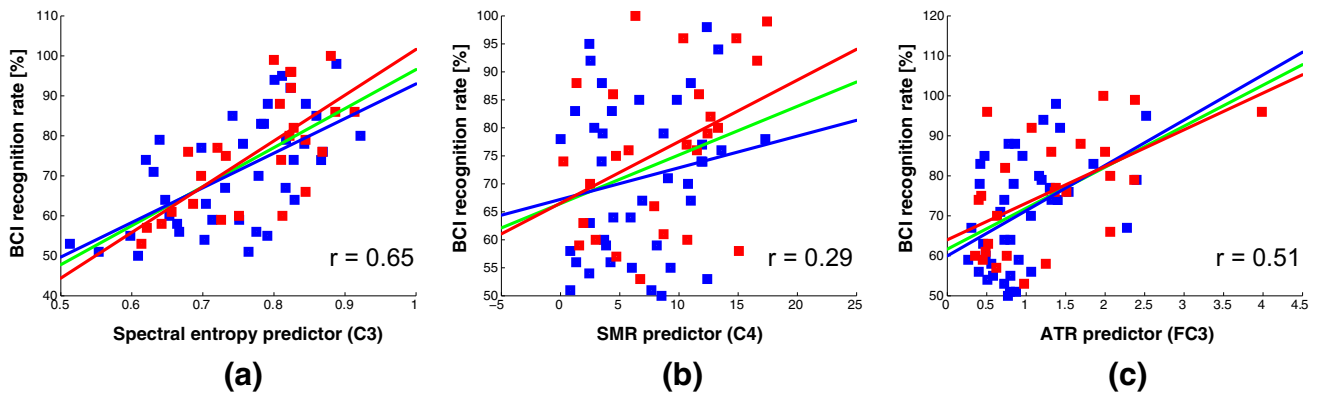
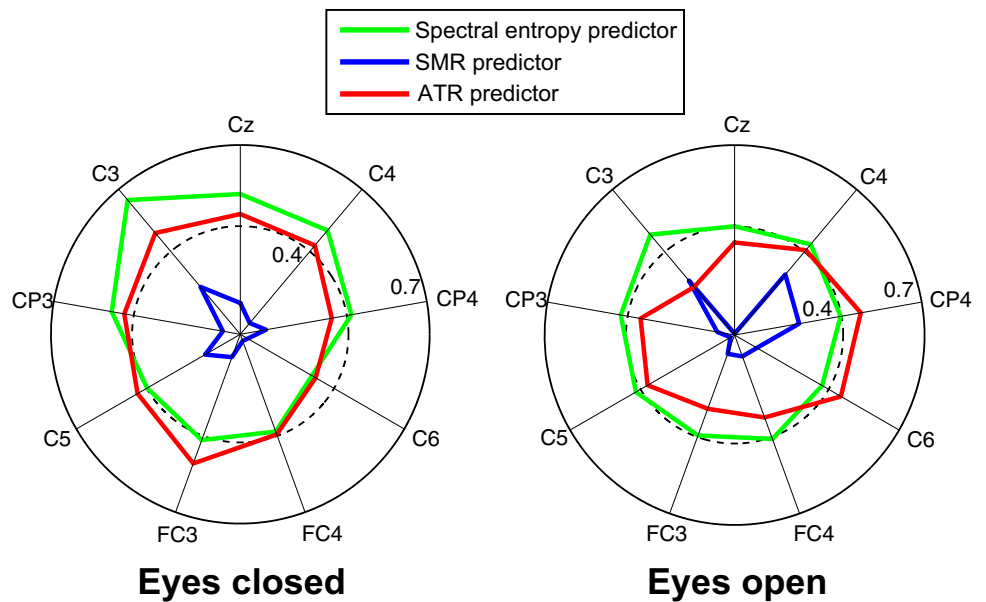
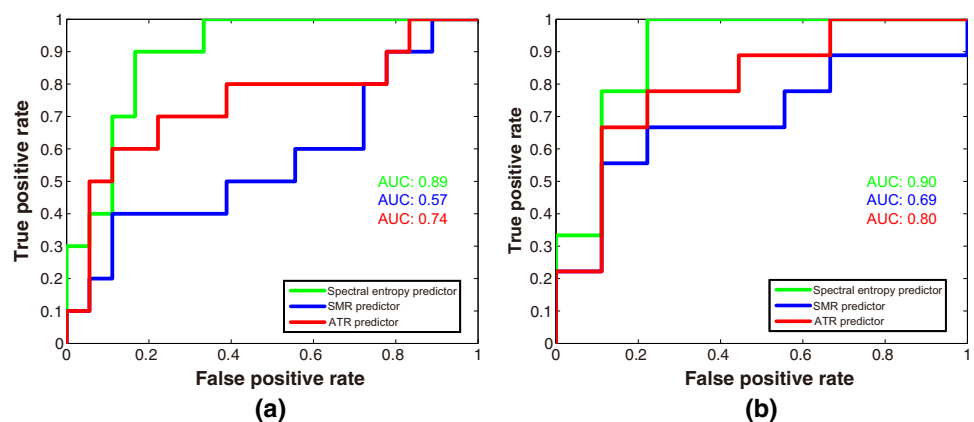


Fig. 5 The relationships between the three predictors and SMR-BCI performance. **a** Spectral entropy predictor; **b** SMR predictor; **c** ATR predictor. *Blue square* subject from the first session; *red square* subject from the second session. *Blue line* denotes the result of linear

regression analysis for the first session, *red line* denotes the result of linear regression analysis for the second session, *green line* denotes the result of linear regression analysis for the merged session (Color figure online)

Fig. 6 ROC curves for the three predictors in classifying the two groups of SMR-BCI users. **a** The first session; **b** the second session. The *horizontal* coordinate denotes the false positive rate, and the *vertical* coordinate denotes the true positive rate. *AUC* area under curve (Color figure online)



the first session, and (0.56, 0.89), (0.67, 0.89) for the second session.

The classification capability was further evaluated by a leave-one-out cross-validation scheme with the prediction-LDA classifier, as described in Sect. 2.4. In the first session, 75, 57 and 71 % classification accuracies were achieved for spectral entropy, SMR, and ATR predictors, respectively. And the accuracies were 89, 61 and 67 % for the second session.

Inter-session Prediction

The 26 subjects who had returned to participate in the second session experiment were selected for the following analysis to investigate the inter-session prediction performance of the proposed predictor. Criteria similar to that mentioned in Sect. 2.4 was used to define the high and low aptitude SMR-BCI user groups.

The inter-session prediction performance was also evaluated using the prediction-LDA classifier, and the classification results were presented in Fig. 7. Figure 7a–c, showed the classification plots of the first session by using the classification boundaries obtained from data of the second session for the spectral entropy, SMR, and ATR

predictors, respectively. The corresponding classification accuracies were 88, 63 and 75 %, with the classification boundaries for the three predictors as 0.77, 8.7 and 1.3. Similarly, the plots of the second session classification for the spectral entropy, SMR, and ATR predictors with the first session as training were shown in Fig. 7d–f, respectively. The corresponding classification accuracies were 89, 50 and 72 %, and the classification boundaries were 0.77, 6.0 and 1.4 for the spectral entropy, SMR, and ATR predictors, respectively.

Consistent Changes in SMR-BCI Performance and Spectral Entropy Predictor

Considering the 26 subjects, 19 of them achieved higher performance in the second session, six of them achieved lower performance in the second session, and equal performance was achieved for the remaining 1 subject. We further investigated whether the increased or decreased change in SMR-BCI performance could be reflected by the predictors obtained from the resting-state EEG. Since there exist normal fluctuations between sessions in SMR-BCI performance, firstly we excluded those subjects whose absolute CP of performance were below 10 %. Finally 10

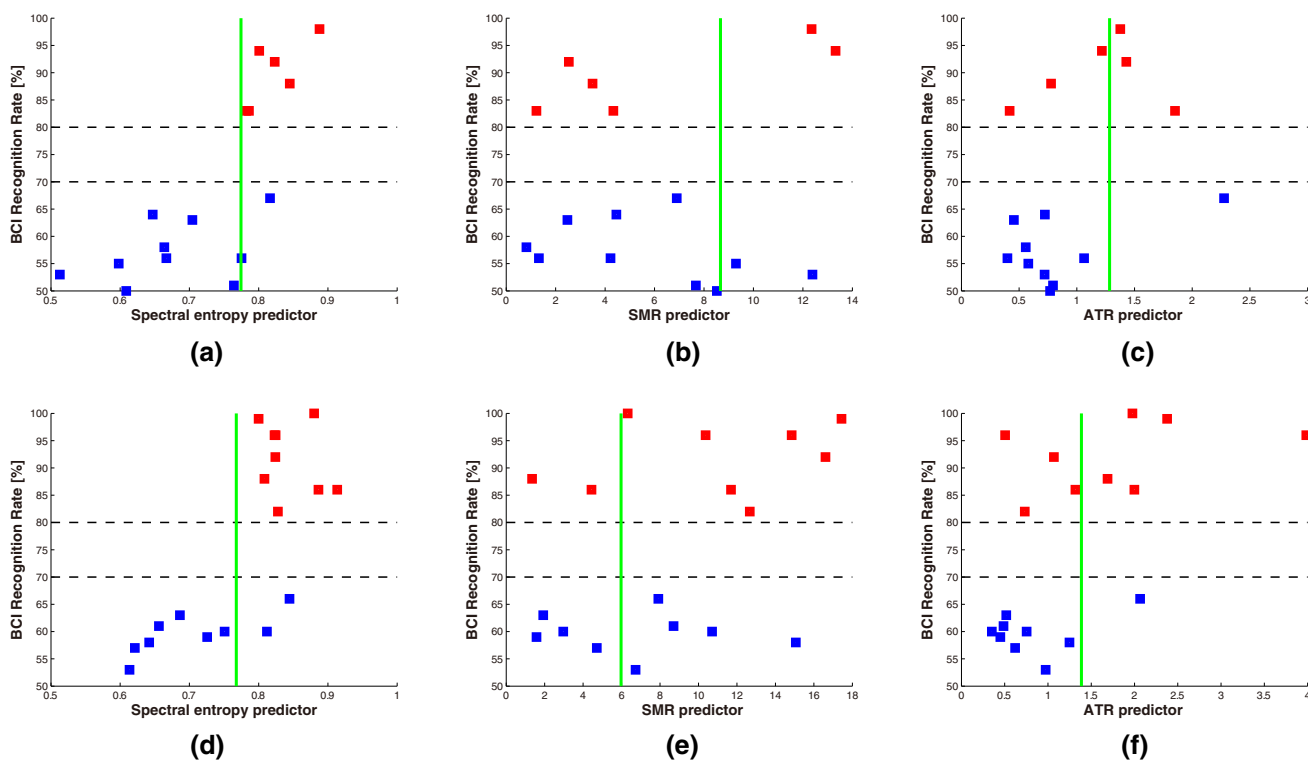


Fig. 7 Inter-session prediction performance. **a** and **d** Spectral entropy predictor; **b** and **e** SMR predictor; **c** and **f** ATR predictor. *Upper panel* the boundary determined from the second session was used to classify the SMR-BCI users in the first session; *bottom panel* the boundary

determined from the first session was used to classify the SMR-BCI users in the second session. *Blue square* denotes the low aptitude SMR-BCI user; *red square* denotes the high aptitude SMR-BCI user; and the *green line* is the classification boundary (Color figure online)

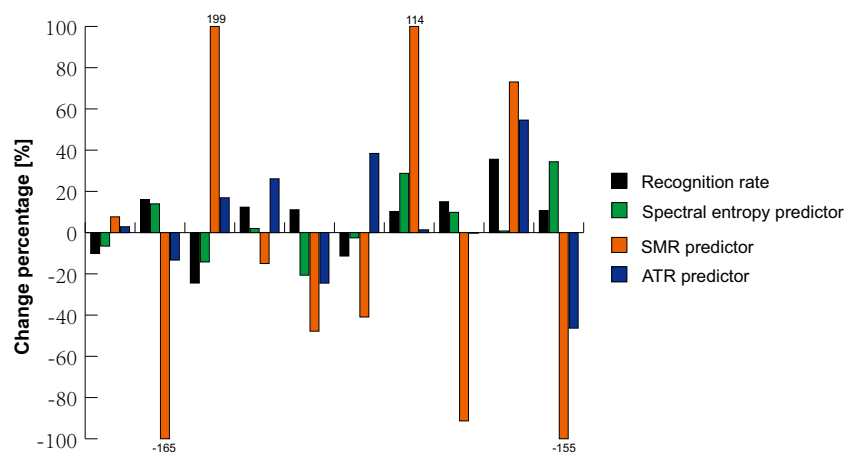
subjects were screened out, and the CP of the SMR-BCI performance and the three predictors between sessions for the 10 subjects were illustrated in Fig. 8. It showed that spectral entropy predictor has a consistent change with SMR-BCI performance for the 9 of 10 subjects. Whereas for SMR and ATR predictors, the corresponding subject numbers were both three.

Discussions

The neural mechanisms of the SMR-BCI performance variations across healthy subjects remain unclear. However, finding a reliable biomarker to predict SMR-BCI performance has great value. Based on previous studies (Ahn et al. 2013; Blankertz et al. 2010), we assumed that the spectral entropy from resting-state EEG may be served as a predictor of SMR-BCI performance.

The spectral entropies of channels from brain regions near the sensorimotor area showed a strong correlation with SMR-BCI performance. Among them, the spectral entropy of channel C3 from the eyes closed resting-state EEG yielded the highest CC ($r = 0.65$, $p < 10^{-8}$) compared with other channels. Since the above results were obtained from the merged session, in which the 26 subjects of the second session were depend on the 40 subjects of the first session, the correlation analysis may be interfered. We further calculated the CCs between SMR-BCI performance and resting-state spectral entropies based on the two separate sessions, the highest CCs were still achieved by channel C3, and they were $r = 0.61$ ($p < 10^{-4}$) and $r = 0.70$ ($p < 10^{-4}$) for the first and second sessions, respectively. The highest CCs of the merged and separate sessions were both achieved on channel C3, and they were close to each other, suggesting the relationship was robust. Therefore, we proposed to use the eyes closed resting-state spectral entropy of channel C3 as an effective predictor for SMR-BCI performance.

Fig. 8 The change percentage (CP) of the recognition rate and the three predictors between the first and second sessions for the 10 subjects whose CP of SMR-BCI recognition rate exceeded 10 %. Note we mark the true CP value if it is higher than 100 % (Color figure online)



SMR-BCI Inefficiency Phenomenon

The SMR-BCI inefficiency phenomenon is one of the biggest challenges in SMR-BCI research because these subjects cannot achieve accurate control of SMR-BCI even after several training sessions (Kübler et al. 2011). According to a report by (Vidaurre and Blankertz 2010), 15–30 % of the users are SMR-BCI inefficiency. This percentage is high enough that the public may become doubtful about the usefulness of SMR-BCI technology. In this case, finding an easy-to-use biomarker has great meaning, those inefficient subjects could be screened out at the beginning. In the current study, the SMR-BCI recognition rate of one subject group is below 70 %, which may be treated as or close to SMR-BCI inefficient subjects.

Note that one subject cannot be easily judged as SMR-BCI inefficiency by only one training session because many factors may lead to a poor SMR-BCI performance at the first time, such as unfamiliarity with the system, unsuitable motor imagery strategies, and nervousness. Stricter criteria will be needed to define truly inefficient subjects in the future study (Blankertz et al. 2010).

Characteristics of the Spectral Entropy Predictor

Spectral entropy measures the uniformity of the power spectral density. On one hand, a signal with a single frequency component (e.g., a pure sinusoid) produces the smallest spectral entropy, on the other hand, a signal with all frequency components of equal power value (e.g., white noise) produces the greatest spectral entropy (Inouye et al. 1991). The power spectrum of the resting-state EEG is usually characterized by obvious peaks and valleys distributed throughout the low frequency band. As for the subjects with different levels of SMR-BCI performance, the obvious resting-state EEG power spectrum difference could be seen in Fig. 9. The peaks located in the alpha rhythm had the highest amplitude for the group of subjects

with recognition rates above 80 %, the lowest amplitude for the group with recognition rates below 70 %, and a middle amplitude for the group with recognition rates between 70 and 80 %. It is known that spectral entropy depends primarily on the number of peaks and their peakness, thus it is powerful for capturing the group differences reflected by the distribution of the EEG power spectrum.

Figure 4 shows that spectral entropy calculated from resting-state EEG data on channel C3 has the highest correlation with SMR-BCI performance, regardless of whether the subjects' eyes were closed or opened. Notably, in the merged session, the corresponding CCs between SMR-BCI performance and the eyes closed resting-state spectral entropy reached 0.65, 0.52 and 0.50 for channels C3, Cz, and C4, respectively. It is well known that the C3, Cz, and C4 channels are located on the sensorimotor areas, thus the higher CCs on these three channels could be explained by the neurophysiological fact that motor imagery-related brain activity dominate in the sensorimotor areas (Neuper et al. 2006). The impressive prediction performance of the C3 spectral entropy is further demonstrated in Figs. 5 and 6, in which the obvious linear trend and the large AUC value are shown. Furthermore, the intra-session classification accuracies were both high for the two separate sessions, highlighting the reliable performance of the spectral entropy predictor in distinguishing the two SMR-BCI user groups. The superiority of the C3 channel over the other channels in SMR-BCI performance prediction may be attributed to the left hemisphere domination for

motor skills (Babiloni et al. 2003; Gao et al. 2011; Rogers et al. 2004).

Figure 4 also shows that the spectral entropy calculated from eyes closed resting-state EEG is superior in predicting the SMR-BCI performance compared with that calculated from eyes open state. Two advantages are gained by collecting resting-state EEG data with eyes closed. Firstly, the electrooculography artifact is excluded from the recording, which is important because the frequency band of the electrooculography artifact overlaps with the frequency band we selected to calculate spectral entropy (Fatourehchi et al. 2007); Secondly, closing the eyes reduces unexpected interference from other cognition activities, which is the primary reason why subjects are asked to close their eyes in most resting-state studies, including both MRI and EEG (Luo et al. 2012; Raichle et al. 2001; Xu et al. 2013b).

Session-to-Session Transfer

EEG signal are not stationary, resulting in changes in spectrum over time. In the current study, the optimal frequency band, spatial filters, and parameters for the decoding-LDA classifier were estimated within session when calculating SMR-BCI performance, in order to alleviate the effect of non-stationary EEG signal. However, the two experimental sessions in this study were conducted with approximately 3 months interval, and it is unknown whether the predictors calculated from one session is transferable to another session, i.e., whether it is possible to predict subject's SMR-BCI performance based on

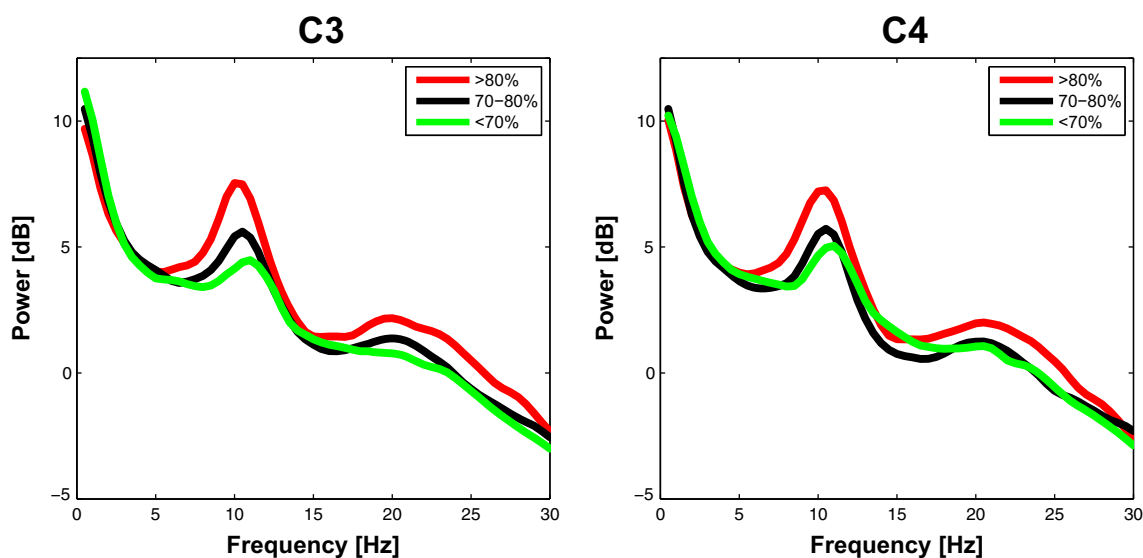


Fig. 9 Average power spectrum of three groups of SMR-BCI users. *Left* power spectrum of channel C3; *right* power spectrum of channel C4. *Red line* denotes the group of users whose SMR-BCI recognition rate are above 80 %; *green line* denotes the group of users whose

SMR-BCI recognition rate are below 70 %; and the *black line* denotes the group of users whose SMR-BCI recognition rate range from 70 to 80 % (Color figure online)

prediction model established from a different session. Inspiringly, Fig. 5a demonstrates that the relationships between SMR-BCI performance and spectral entropy predictor are similar between the two sessions.

One of the key merits of the spectral entropy predictor is that it measures the probability distribution of the PSD. In the different sessions, the absolute power spectrum of resting-state EEG data may change over time, but the probability distribution of the PSD may remain relatively stable. The classification results shown in Fig. 7 demonstrate that the spectral entropy predictor is reliable in distinguishing the two SMR-BCI user groups based on the prediction model estimated from a different session. More importantly, the classification boundaries for the high and low aptitude SMR-BCI user groups obtained from the two different sessions are close to each other. The above result also implies that it is possible to determine a threshold from the proposed spectral entropy predictor to classify SMR-BCI novice users as either high or low aptitude SMR-BCI users.

For the same subject, the SMR-BCI recognition rates obtained between sessions are generally different, and CP above 10 % are found for 10 of the 26 subjects. Then whether the SMR-BCI performance changes can be reflected by the changes in the spectral entropy predictor becomes a noteworthy issue. We further investigate this problem, and the results are shown in Fig. 8. For 9 of the 10 subjects, SMR-BCI performance increases (decreases) with the increase (decrease) of the spectral entropy predictor. The CP values of spectral entropy predictor are usually lower than SMR-BCI recognition rates.

SMR, ATR, and Spectral Entropy Predictors

Among the three predictors, spectral entropy predictor achieves the best prediction performance, ATR predictor performs well, whereas the performance of SMR predictor is not good enough. We think the explanation of the differences could be found from the definitions of the three predictors: SMR predictor reflects the peakness of the spectrum; ATR predictor involves alpha and theta bands information and equals to the ratio of them; spectral entropy predictor utilizes the probability information of the spectrum and measures the uniformity of the power spectral density. Compared with SMR and ATR, spectral entropy utilizes a kind of statistical measure to denote the power spectrum, which may be more robust to reduce noise effect. In addition, the absolute peakness and band powers of the resting-state spectrum may be different from person and person, and may depend on age and sex (Mundy-Castle 1951; Richard Clark et al. 2004), thus SMR and ATR predictors may be influenced. However, spectral entropy is a measure based on probability, and it has been proved to

be more stable across subjects in previous studies (Nunes et al. 2004; Rezek and Roberts 1998).

Limitations

Limitations of this study is that we do not know whether the proposed spectral entropy predictor could be transferred from healthy subjects to patient populations such as amyotrophic lateral sclerosis (ALS) and stroke. Because diseases may have profound and system-wide effects that may eliminate or even reverse effects found in healthy populations (Grosse-Wentrup and Schölkopf 2013).

Conclusions

Understanding the inter-subject SMR-BCI performance variation is one of the fundamental problems in SMR-BCI application. In this study, we established an effective spectral entropy predictor for SMR-BCI performance, which derived from 2 min eyes closed resting-state EEG. The proposed predictor provides outstanding classification capability for high and low aptitude BCI users in both intra- and inter-session conditions. To our knowledge, this is the first study that discussed about the reliability of inter-session prediction. The proposed predictor could help to identify subject's potential SMR-BCI performance at the very beginning, avoiding the frustrating and costly training procedures for those low aptitude users.

Acknowledgments This work was supported in part by grants from the 973 program 2011CB707803, the National Natural Science Foundation of China (#61175117, #81330032, #31200857 and #31100745), the program for New Century Excellent Talents in University (#NCET-12-0089), the 863 project 2012AA011601, and the National Science & Technology Pillar Program 2012BAI16B02.

Conflict of interest The authors declare that they have no conflict of interest.

Ethical standard All procedures performed in studies involving human participants were in accordance with the ethical standards of Institution Research Ethics Board of the University of Electronic Science and Technology of China, and with the 1964 Helsinki declaration and its later amendments or comparable ethical standards.

Informed consent Informed consent was obtained from all individual participants included in the study.

References

- Ahn M, Cho H, Ahn S, Jun SC (2013) High theta and low alpha powers may be indicative of bci-illiteracy in motor imagery. *PLoS One* 8:e80886. doi:10.1371/journal.pone.0080886
- Babiloni C, Carducci F, Del Gratta C, Demartin M, Romani GL, Babiloni F, Rossini PM (2003) Hemispherical asymmetry in human SMA during voluntary simple unilateral movements. *An*

- fMRI study. *Cortex* 39:293–305. doi:[10.1016/S0010-9452\(08\)70110-2](https://doi.org/10.1016/S0010-9452(08)70110-2)
- Blankertz B et al (2010) Neurophysiological predictor of SMR-based BCI performance. *Neuroimage* 51:1303–1309. doi:[10.1016/j.neuroimage.2010.03.022](https://doi.org/10.1016/j.neuroimage.2010.03.022)
- Clark CR, Veltmeyer MD, Hamilton RJ, Simms E, Paul R, Hermens D, Gordon E (2004) Spontaneous alpha peak frequency predicts working memory performance across the age span. *Int J Psychophysiol* 53:1–9. doi:[10.1016/j.ijpsycho.2003.12.011](https://doi.org/10.1016/j.ijpsycho.2003.12.011)
- Daly JJ, Wolpaw JR (2008) Brain-computer interfaces in neurological rehabilitation. *Lancet Neurol* 7:1032–1043. doi:[10.1016/S1474-4422\(08\)70223-0](https://doi.org/10.1016/S1474-4422(08)70223-0)
- Donchin E, Spencer K, Wijesinghe R (2000) The mental prosthesis: assessing the speed of a P300-based brain-computer interface. *IEEE Trans Rehabil Eng* 8:174–179. doi:[10.1109/86.847808](https://doi.org/10.1109/86.847808)
- Fatourechi M, Bashashati A, Ward RK, Birch GE (2007) EMG and EOG artifacts in brain computer interface systems: a survey. *Clin Neurophysiol* 118:480–494. doi:[10.1016/j.clinph.2006.10.019](https://doi.org/10.1016/j.clinph.2006.10.019)
- Gao Q, Duan X, Chen H (2011) Evaluation of effective connectivity of motor areas during motor imagery and execution using conditional Granger causality. *Neuroimage* 54:1280–1288. doi:[10.1016/j.neuroimage.2010.08.071](https://doi.org/10.1016/j.neuroimage.2010.08.071)
- Gongora M, Peressutti C, Machado S, Teixeira S, Velasques B, Ribeiro P (2013) Progress and prospects in neurorehabilitation: clinical applications of stem cells and brain-computer interface for spinal cord lesions. *Neuro Sci* 34:427–433. doi:[10.1007/s10072-012-1232-5](https://doi.org/10.1007/s10072-012-1232-5)
- Grosse-Wentrup M, Schölkopf B (2012) High gamma-power predicts performance in sensorimotor-rhythm brain-computer interfaces. *J Neural Eng* 9:046001. doi:[10.1088/1741-2560/9/4/046001](https://doi.org/10.1088/1741-2560/9/4/046001)
- Grosse-Wentrup M, Schölkopf B (2013) A review of performance variations in SMR-based brain-computer interfaces (BCIs). In: Guger C, Allison BZ, Edlinger G (eds) *Brain-computer interface research. springerbriefs in electrical and computer engineering*. Springer, Berlin, pp 39–51. doi:[10.1007/978-3-642-36083-1_5](https://doi.org/10.1007/978-3-642-36083-1_5)
- Guger C, Edlinger G, Harkam W, Niedermayer I, Pfurtscheller G (2003) How many people are able to operate an EEG-based brain-computer interface (BCI)? *IEEE Trans Neural Syst Rehabil Eng* 11:145–147. doi:[10.1109/TNSRE.2003.814481](https://doi.org/10.1109/TNSRE.2003.814481)
- Halder S et al (2011) Neural mechanisms of brain-computer interface control. *Neuroimage* 55:1779–1790. doi:[10.1016/j.neuroimage.2011.01.021](https://doi.org/10.1016/j.neuroimage.2011.01.021)
- Halder S, Varkuti B, Bogdan M, Kübler A, Rosenstiel W, Sitaram R, Birbaumer N (2013) Prediction of brain-computer interface aptitude from individual brain structure. *Front Hum Neurosci* 7:105. doi:[10.3389/fnhum.2013.00105](https://doi.org/10.3389/fnhum.2013.00105)
- Hammer EM et al (2012) Psychological predictors of SMR-BCI performance. *Biol Psychol* 89:80–86. doi:[10.1016/j.biopsycho.2011.09.006](https://doi.org/10.1016/j.biopsycho.2011.09.006)
- Inouye T et al (1991) Quantification of EEG irregularity by use of the entropy of the power spectrum. *Electroencephalogr Clin Neurophysiol* 79:204–210. doi:[10.1016/0013-4694\(91\)90138-T](https://doi.org/10.1016/0013-4694(91)90138-T)
- Kübler A, Blankertz B, Müller K, Neuper C (2011) A model of BCI-control. In: *Proceedings of the 5th international brain-computer interface conference*. Graz University of Technology, Austria, pp 100–103
- Li Y, Long J, Yu T, Yu Z, Wang C, Zhang H, Guan C (2010) An EEG-based BCI system for 2-D cursor control by combining Mu/Beta rhythm and P300 potential. *IEEE Trans Biomed Eng* 57:2495–2505. doi:[10.1109/TBME.2010.2055564](https://doi.org/10.1109/TBME.2010.2055564)
- Lotte F, Guan C (2011) Regularizing common spatial patterns to improve BCI designs: unified theory and new algorithms. *IEEE Trans Biomed Eng* 58:355–362. doi:[10.1109/TBME.2010.2082539](https://doi.org/10.1109/TBME.2010.2082539)
- Lu J, McFarland DJ, Wolpaw JR (2012) Adaptive Laplacian filtering for sensorimotor rhythm-based brain-computer interfaces. *J Neural Eng* 10:016002. doi:[10.1088/1741-2560/10/1/016002](https://doi.org/10.1088/1741-2560/10/1/016002)
- Luo C et al (2012) Resting state basal ganglia network in idiopathic generalized epilepsy. *Hum Brain Mapp* 33:1279–1294. doi:[10.1002/hbm.21286](https://doi.org/10.1002/hbm.21286)
- Müller-Gerking J, Pfurtscheller G, Flyvbjerg H (1999) Designing optimal spatial filters for single-trial EEG classification in a movement task. *Clin Neurophysiol* 110:787–798. doi:[10.1016/S1388-2457\(98\)00038-8](https://doi.org/10.1016/S1388-2457(98)00038-8)
- Mundy-Castle AC (1951) Theta and beta rhythm in the electroencephalograms of normal adults. *Electroencephalogr Clin Neurophysiol* 3:477–486
- Neuper C, Wörtz M, Pfurtscheller G (2006) ERD/ERS patterns reflecting sensorimotor activation and deactivation. *Prog Brain Res* 159:211–222. doi:[10.1016/S0079-6123\(06\)59014-4](https://doi.org/10.1016/S0079-6123(06)59014-4)
- Nunes RR, Almeida MP, Sleight JW (2004) Spectral entropy: a new method for anesthetic adequacy. *Rev Bras Anestesiol* 54:404–422
- Raichle ME, MacLeod AM, Snyder AZ, Powers WJ, Gusnard DA, Shulman GL (2001) A default mode of brain function. *Proc Natl Acad Sci U S A* 98:676–682. doi:[10.1073/pnas.98.2.676](https://doi.org/10.1073/pnas.98.2.676)
- Rezek IA, Roberts SJ (1998) Stochastic complexity measures for physiological signal analysis. *IEEE Trans Biomed Eng* 45:1186–1191. doi:[10.1109/10.709563](https://doi.org/10.1109/10.709563)
- Rogers BP, Carew JD, Meyerand ME (2004) Hemispheric asymmetry in supplementary motor area connectivity during unilateral finger movements. *Neuroimage* 22:855–859. doi:[10.1016/j.neuroimage.2004.02.027](https://doi.org/10.1016/j.neuroimage.2004.02.027)
- Vidaurre C, Blankertz B (2010) Towards a cure for BCI illiteracy. *Brain Topogr* 23:194–198. doi:[10.1007/s10548-009-0121-6](https://doi.org/10.1007/s10548-009-0121-6)
- Vidaurre C, Kawanabe M, von Bunau P, Blankertz B, Müller K-R (2011) Toward unsupervised adaptation of LDA for brain-computer interfaces. *IEEE Trans Biomed Eng* 58:587–597. doi:[10.1109/TBME.2010.2093133](https://doi.org/10.1109/TBME.2010.2093133)
- Vuckovic A, Osuagwu BA (2013) Using a motor imagery questionnaire to estimate the performance of a brain-computer interface based on object oriented motor imagery. *Clin Neurophysiol* 124:1586–1595. doi:[10.1016/j.clinph.2013.02.016](https://doi.org/10.1016/j.clinph.2013.02.016)
- Wang Y, Wang R, Gao X, Hong B, Gao S (2006) A practical VEP-based brain-computer interface. *IEEE Trans Neural Syst Rehabil Eng* 14:234–239. doi:[10.1109/TNSRE.2006.875576](https://doi.org/10.1109/TNSRE.2006.875576)
- Wolpaw JR, McFarland DJ (2004) Control of a two-dimensional movement signal by a noninvasive brain-computer interface in humans. *Proc Natl Acad Sci U S A* 101:17849–17854. doi:[10.1073/pnas.0403504101](https://doi.org/10.1073/pnas.0403504101)
- Wolpaw JR, Birbaumer N, McFarland DJ, Pfurtscheller G, Vaughan TM (2002) Brain-computer interfaces for communication and control. *Clin Neurophysiol* 113:767–791. doi:[10.1016/S1388-2457\(02\)00057-3](https://doi.org/10.1016/S1388-2457(02)00057-3)
- Xu P, Hu X, Yao D (2013a) Improved wavelet entropy calculation with window functions and its preliminary application to study intracranial pressure. *Comput Biol Med* 43:425–433. doi:[10.1016/j.compbiomed.2013.01.022](https://doi.org/10.1016/j.compbiomed.2013.01.022)
- Xu P et al (2013b) Cortical network properties revealed by SSVEP in anesthetized rats. *Sci Rep* 3:2496. doi:[10.1038/srep02496](https://doi.org/10.1038/srep02496)
- Xu P, Liu T, Zhang R, Zhang Y, Yao D (2014) Using particle swarm to select frequency band and time interval for feature extraction of EEG based BCI. *Biomed Signal Process Control* 10:289–295. doi:[10.1016/j.bsp.2013.08.012](https://doi.org/10.1016/j.bsp.2013.08.012)
- Zhang R, Xu P, Guo L, Zhang Y, Li P, Yao D (2013) Z-score linear discriminant analysis for EEG based brain-computer interfaces. *PLoS One* 8:e74433. doi:[10.1371/journal.pone.0074433](https://doi.org/10.1371/journal.pone.0074433)